C. R. Physique 11 (2010) 397–404

Contents lists available at ScienceDirect

Comptes Rendus Physique

www.sciencedirect.com

Optical properties of nanotubes / Propriétés optiques des nanotubes

Evaluation of sorted semi-conducting carbon nanotube films for gas sensing applications

Évaluation des films de nanotubes de carbone tries semi-conducteurs pour application aux capteurs de gaz

Yann Battie [a], Olivier Ducloux [b,*], Philippe Thobois [a], Yannick Coffinier [c], Annick Loiseau [b]

[a] *LEM ONERA – CNRS UMR 104, 29, avenue de la Division Leclerc, 92322 Châtillon cedex, France*
[b] *ONERA – DMPH, 29, avenue de la Division Leclerc, 92322 Châtillon cedex, France*
[c] *IRI CNRS USR 3078, avenue Poincaré, 59652 Villeneuve d'Ascq, France*

ARTICLE INFO

Article history:
Available online 19 August 2010

Keywords:
Carbon nanotubes
Nanotube sorting
Ultracentrifugation
Nanostructures
Gas sensors
Microsensors

Mots-clés :
Nanotubes de carbone
Tri de nanotubes
Ultracentrifugation
Nanostructures
Capteurs de gaz
Micro-capteurs

ABSTRACT

This work focuses on the elaboration of sorted semi-conducting single walled carbon nanotube films (SC-SWCNT films), and the evaluation of a gas microsensor based on these films. First, we show that semi-conducting carbon nanotubes could be sorted from solutions containing both metallic and semi-conducting nanotubes by ultracentrifugation in a density gradient. SC-SWCNT films were then obtained by filtration through a nitrocellulose membrane, then transferred on TLM (transmission line method) electrodes to separately measure the resistivity and the contact resistance. We finally show characterization results obtained using NO_2 and NH_3 as a target gas.

RÉSUMÉ

Le travail présenté concerne l'élaboration de films de nanotubes de carbone monoparoi triés semi-conducteurs (SC-SWCNT), ainsi que la caractérisation de micro-capteurs de gaz fabriqués sur la base de ces derniers. Nous exposons d'abord la méthode de centrifugation dans un gradient de densité utilisée pour trier les CNT semi-conducteurs des CNT métalliques. Des films de SC-SWCNT sont ensuite obtenus par filtration à travers une membrane en nitrocellulose, puis transférés sur des électrodes de type TLM (*transmission line method*) pour évaluer séparément leur résistivité et leur résistance de contact. Les résultats de caractérisation sur NO_2 et NH_3 sont enfin présentés.

1. Introduction

Since their discovery by IIjima et al. in 1991, much research has been conducted on carbon nanotubes (CNT) and related carbon-based nanomaterials. Carbon nanotubes, composed exclusively of surface atoms, show a high sensitivity to their environment. Dai et al. [1] were the first to use carbon nanotubes as a base material for gas sensing applications, stressing on their high sensitivity, but low selectivity. Many other research works have been conducted so far on CNT-based gas sensors

* Corresponding author.
E-mail address: Olivier.ducloux@onera.fr (O. Ducloux).

1631-0705/$ – see front matter
doi:10.1016/j.crhy.2010.06.004

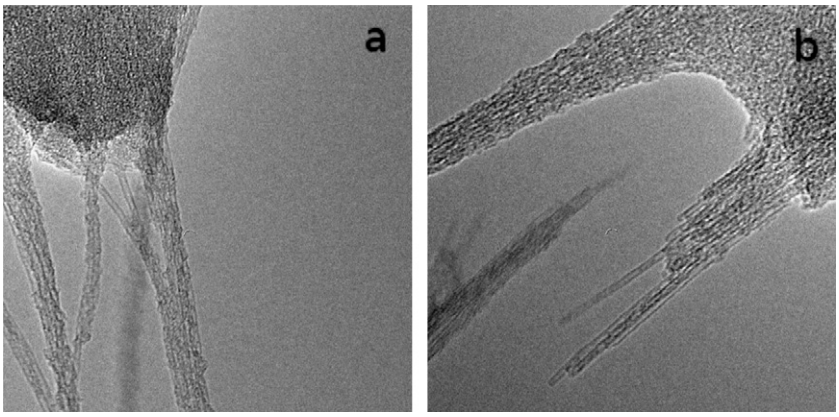

Fig. 1. TEM pictures of (a) unsorted SWCNT and (b) sorted SWCNT.

[2,3], employing different strategies to increase the selectivity of the studied sensors. Using polymer functionalization [4] the authors could reduce the response to NH_3 or NO_2 by using respectively Nafion or polyethyleneimine (PEI) coatings. Following another lead, others showed that nanotube decoration using metallic nanoparticles [5] allows sensing of other types of gases such as hydrogen.

As a proof of the potential of the CNT-based sensor technology, CNT-based gas and biosensor technologies reached the industrial scale, NANOMIX being the major actor in this field.

Interestingly, the comprehension of the physics of the CNT/gas molecule interaction has not reached a consensus yet. The sensitivity of CNT to gas molecules is currently explained by two theories. The generally accepted mechanism is chemical doping on the surface of carbon nanotubes involving charge transfer between gas molecules and p-doped carbon nanotubes. This mechanism is consistent with the evolution of the resistivity upon exposure to an electron donor or acceptor gas, respectively NO_2 and NH_3, and was confirmed by ab-initio calculations. On the other hand, Bondavalli et al. interpret the response of CNT-based gas sensors by a different mechanism: a modification of the Schottky contact between the semi-conducting nanotubes and the electrical contacts [6]. Using this approach, and varying the electrode metal, the authors reported a matrix of CNT-based gas sensors aiming at the analysis of complex atmospheres by recognition of different gas fingerprints.

In this work, we chose to play on the nanotubes themselves as a way of improving the sensitivity to CNT-based gas sensors. To do so, we first focused on the CNT sorting operation, recently demonstrated by Hersam et al. [7] using density gradient ultracentrifugation (DGU). The sorted nanotubes were then structured in films and transferred onto electrodes for resistivity measurements. The transmission line method (TLM) was used to monitor separately the resistivity of the films and the contact resistance. In this article, we will first expose the sorting method used, and characterization of the sorted nanotubes. The second part of the article focuses on the characterization of the fabricated sensors using NO_2 and NH_3 as a target gas.

2. Sorting of nanotubes

Single walled carbon nanotubes (SWCNT) are purchased from Carbon Solutions, Inc., California. They are obtained by electric arc discharge and are composed of 70–90% SWCNT. The mean diameter of SWCNT is estimated from transmission electron microscopy (TEM) at 1.35 nm (Fig. 1a).

SWCNT are dispersed in an aqueous solution as follows: 40 mg of SWCNT are dispersed in 10 ml of water with 2% w/v sodium cholate (Sigma-Aldrich, Inc.). The dispersion is sonicated using an ultrasonic tip at 240 W for 1 h. The resulting solution is centrifuged at 160 000*g* for 1 h with a Beckmann Coulter SW41 rotor. A precipitate is formed at the bottom of the centrifuged tube. This preliminary selection step allows the removal of the heaviest particles. The supernatant is then collected. It consists of a homogeneous opaque solution composed of semi-conducting and metallic SWCNT. In order to sort semi-conducting single walled carbon nanotubes (SC-SWCNT), we propose to use the density gradient ultracentrifugation process developed by M.C. Hersam [7].

Aqueous dilutions of iodixanol containing 1.4% w/v sodium cholate and 0.6% w/v sodium dodecyl sulfate (Sigma-Aldrich, Inc.) are used as a density gradient media. A linear mass density gradient ranging from 1.08 to 1.19 is then formed in a centrifuge tube by using a linear gradient maker. After the formation of the gradient, 1.5 ml of 60% w/v iodixanol is added at the bottom of the centrifuge tube. 1.8 ml of a solution composed of SWCNT supernatant mixed with iodixanol (27.5% w/v) is injected into the bottom of the gradient. The top of the tube is filled with an aqueous solution containing 1.4% w/v of sodium cholate and 0.6% w/v of sodium dodecyl sulfate.

This preparation is then centrifuged for 14 h at 160 000*g*. After this step, a pink layer is clearly observed at the top of the density gradient. This layer is collected using a flat opened needle.

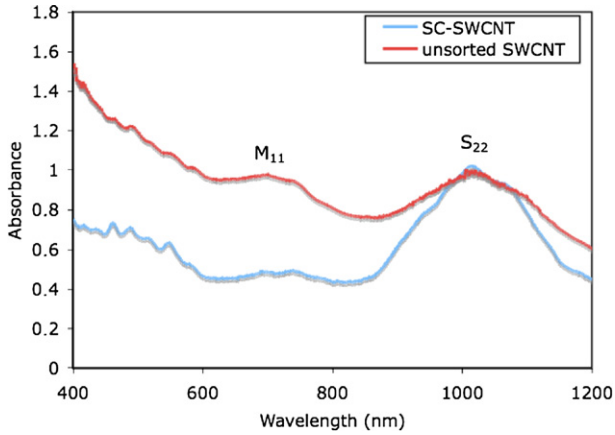

Fig. 2. Normalized UV–vis–IR spectra of the unsorted SWCNT and sorted SWCNT.

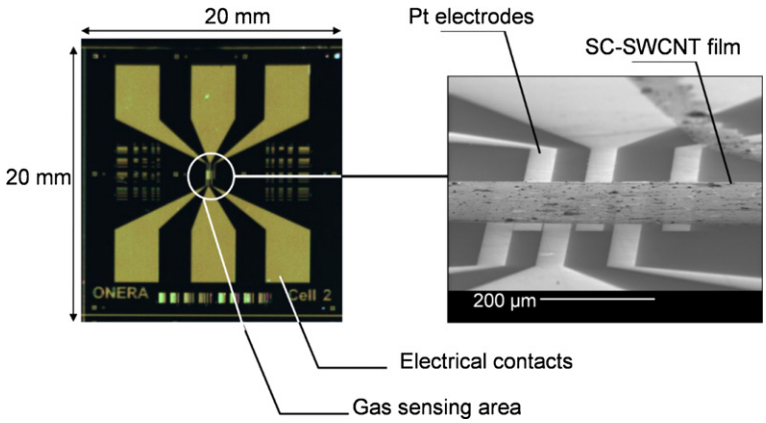

Fig. 3. Architecture of the sensor, comprising TLM electrodes and the SC-SWCNT film.

Normalized UV–vis–IR spectra of the collected layer and of the unsorted SWCNT are reported in Fig. 2. The spectrum of the unsorted SWCNT presents two broad bands centred at 1015 nm for E_{22} and 710 nm for M_{11}. These bands are also observed at the same wavelengths in the spectrum of the sorted sample. The band position essentially depends on the tube diameter. This result means that the diameter of the SWCNT does not vary during the procedure. The mean diameter of SWCNT is estimated from absorption spectra at 1.4 nm [8]. It is in accordance with the diameter distributions obtained by TEM microscopy (Fig. 1a, b).

The amplitude ratio between the E_{22} and the M_{11} bands can be used to estimate the relative concentration of SC-SWCNT in the samples [7]. The unsorted sample and the sorted sample are respectively composed of 67% and 93% of SC-SWCNT. It confirms that the sorted sample is enriched in SC-SWCNT by enhancing the mass differences between the tubes by a specific non-covalent adsorption of surfactants.

The SC-SWCNT film is obtained by filtration of the sorted SC-SWCNT solution through a nitrocellulose membrane (pore size 200 nm).

3. Microsensor design and fabrication

In order to monitor separately the resistivity and the contact resistance of the nanotubes, the transmission line method (TLM) was used. The microsensor architecture is presented in Fig. 3. It consists of six platinum electrodes deposited on an insulating layer, covered by a film of sorted SC-SWCNT. Platinum is chosen for its temperature stability and for its chemical inertness.

The fabrication process is presented in Fig. 4. First of all, undoped silicon substrates are covered by a 200 nm thick layer of thermal oxide to provide electrical insulation. An 80 nm Pt layer is then deposited by sputtering and patterned by lift-off to fabricate the electrodes. Adhesion of the metal on the SiO_2 insulation layer is obtained by etching prior to deposition during 30 s at 200 W.

The SC-SWCNT films are finally transferred onto the electrodes. This operation is realized by dissolution of the nitrocellulose membrane bearing the CNT film in acetone.

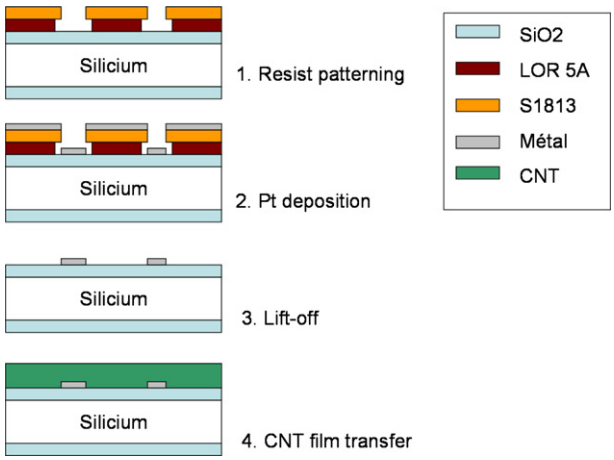

Fig. 4. Fabrication process of the gas sensor.

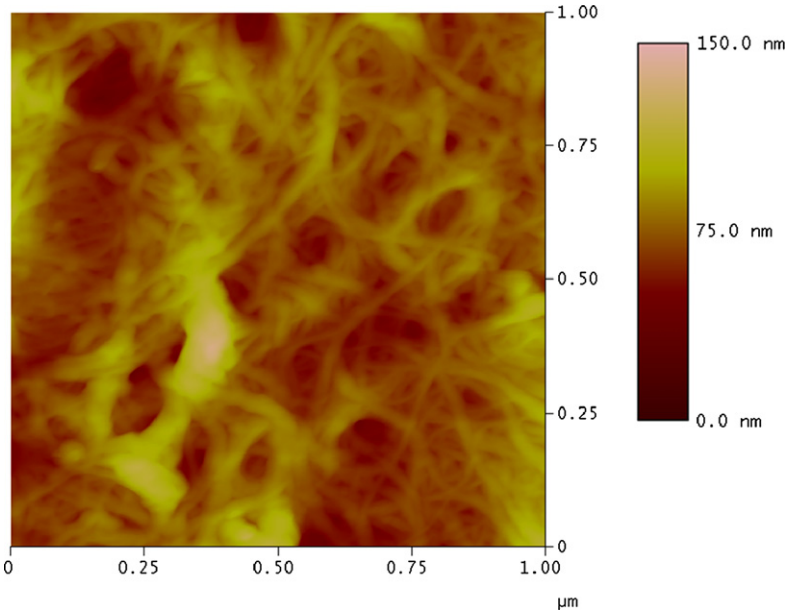

Fig. 5. AFM image of the nanotube film after transfer on the electrodes.

AFM topology of the deposited nanotubes reveals a continuous film. The AFM studies also reveal the presence of a few bundles in the film. An AFM image of the SC-SWCNT film is presented in Fig. 5.

The microsensor is connected to the electrical measurement unit (Keithley 2601 Source Meter) by electrically soldering 50 µm diameter gold wires on the Pt contact pads. The mechanical stability of the soldered contacts was successfully tested up to 300 °C.

4. Characterization

4.1. Drift and stabilization

The sensors were first annealed in air in order to remove residual water, iodixanol and surfactant [9] and stabilize the sensor drift. A large drop of the sensor resistance (−50% to −70%) was measured after a first annealing at 300 °C during 2 h, with a stabilization during the following annealings at 200 °C and 150 °C, as shown in Fig. 6.

This effect is attributed to the evaporation of water and to the pyrolysis of iodixanol and surfactant during the annealing, providing a better contact between nanotubes in the film and improving the nanotube/electrode contact: a small decrease of the measured contact resistance could be noticed, as shown in Fig. 7.

An interesting feature is the TLM analysis of the film characteristics. As can be seen in Fig. 7, the stabilization annealing induces the modification of the linear curve initially measured on the CNT film before annealing. Compared to the linear fit,

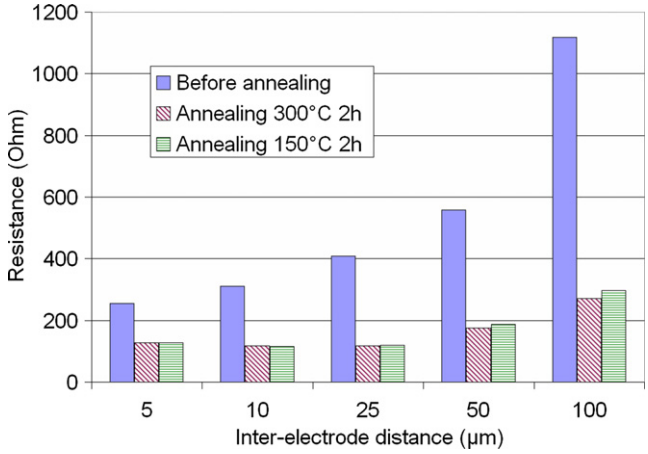

Fig. 6. Measured resistance before and after annealing.

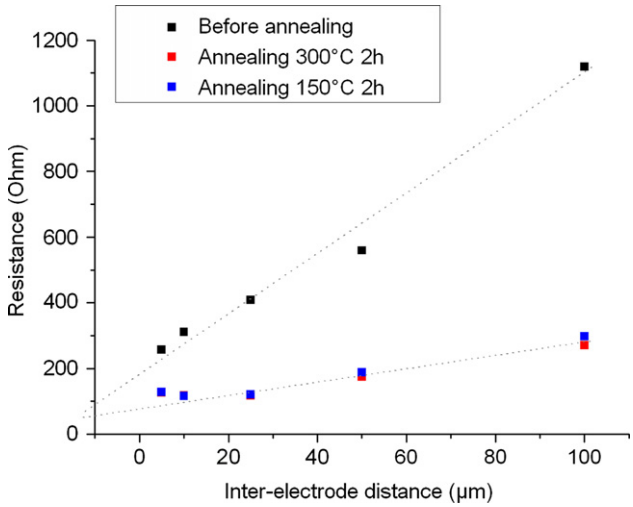

Fig. 7. TLM analysis of the SC-SWCNT film resistance before and after annealing.

a higher resistance is measured for both of the two lower inter-electrode spacings. This effect is also noticed on unsorted nanotube films. It was not observed in [10] because the inter-electrode distances used are larger than ours. The resistance measured when the inter-electrode distance is less than 10 µm [6] is mainly attributed to ballistic transport in metallic nanotubes [11].

Finally, the sensitivity of the deposited nanotube film to temperature was evaluated. A small mean temperature dependence of the resistance, ranging from 0.04 to 0.13%/°C was measured on the five electrode spacings. Hopefully, as will be discussed in the next section, the sensor response to a temperature variation of 1 °C is two orders of magnitude smaller than the response to 1 ppm NO_2 or NH_3 (electrode spacing of 100 µm).

4.2. Gas sensing

For the gas sensing, the SC-SWCNT sensor was loaded in a chamber and then N_2 purged at 100 °C for 15 min in order to remove any traces of water. N_2 was used as the base gas while NH_3 and NO_2 were used to test the sensor sensitivity. Each NH_3 or NO_2 exposure is carried out during 30 min at room temperature and at 1100 mbar. The desorption of NH_3 lasted for 30 min at 100 °C under a N_2 flow. In the case of NO_2, this temperature is not sufficient to remove all adsorbed molecules. For NO_2, the sensor recovery was carried out at 200 °C under vacuum (2×10^{-2} mbar).

The variation of resistance during the adsorption and desorption of gas for an inter-electrode distance equal to 50 µm is represented in Fig. 8. The influence of the gas concentration on the sensor sensitivity is reported in the insert of Fig. 9. The sensitivity to NO_2 is 10 times larger then the sensitivity to NH_3. To the best of our knowledge, the sensitivity is similar to the sensitivity obtained in the literature. Currently, the sensor is able to detect less than 600 ppb of NH_3 and NO_2. This limitation is attributed to the experimental set up and some new investigations are in progress. The response time of the

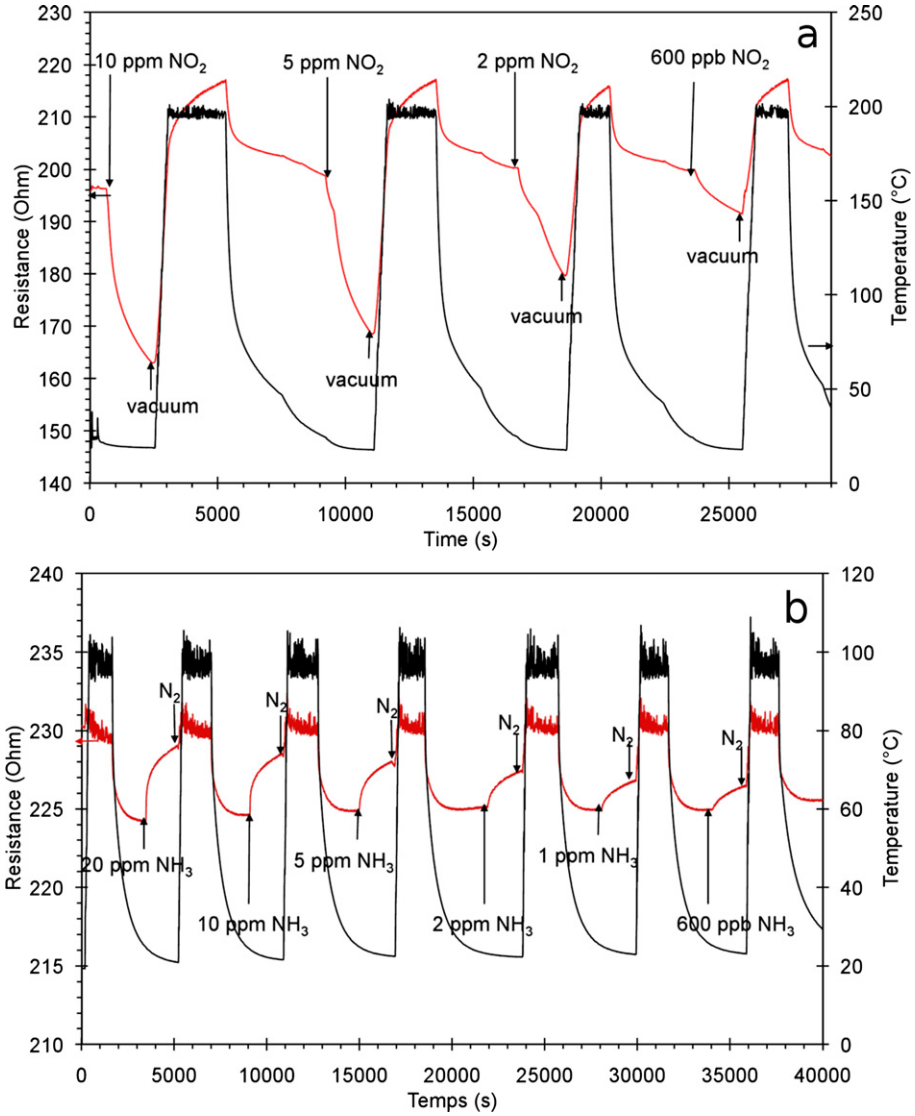

Fig. 8. Variation of resistance during (a) a NO_2 and (b) a NH_3 gas exposure followed by a gas desorption.

sensor is estimated at 15–25 min. The base line resistance (i.e. the resistance in a nitrogen atmosphere) is repeatable and stable during cycles. This reflects a complete desorption of gas molecules during the sensor recovery.

According to previous observations [12], the measured resistance of the SC-SWCNT film rises when the sensor is exposed to NH_3 while it decreases during a NO_2 exposure. In parallel, the sensitivity to NH_3 rises with the concentration until it reaches 50 ppm (Fig. 9). This saturation is also observed for the smallest inter-electrode distance in the case of a NO_2 exposure. Starting from this concentration, all NH_3 adsorption sites are saturated. The sensor sensitivity increases with the inter-electrode distance, which is in accordance to a cumulative gas effect. The contact resistance measured by TLM analysis (Fig. 9) is independent of the gas concentration. Only the intrinsic resistance of the SC-SWCNT film is modified during the gas exposure. It means that the Schottky barrier is not affected by the gas adsorption. From these results, we can assume that the gas adsorption on the SC-SWCNT is the main mechanism leading to the gas detection.

NO_2 bears an unpaired electron and is known as a strong oxidizer. The electron charge transfer is likely to occur from the p-type SC-SWCNTs to NO_2. The concentration of the hole charge carriers increases causing a decrease of resistance. The opposite effect is observed with NH_3 which is an electron donor gas. However, further study leaded by C.W. Bauschlicher et al. [13] has showed that the adsorption of a NH_3 molecule on a SWCNT involves only 0.008 electrons per molecule while the maximum binding energy of NH_3 to a SWCNT is about 0.087 eV. So, the sensor is less sensitive to NH_3 than NO_2. In the case of NH_3, the binding is mostly electrostatic in nature. By comparing the temperature necessary to desorb NO_2 and NH_3, we can conclude that NH_3 is preferentially physisorbed while NO_2 is directly chemisorbed on the SC-SWCNT.

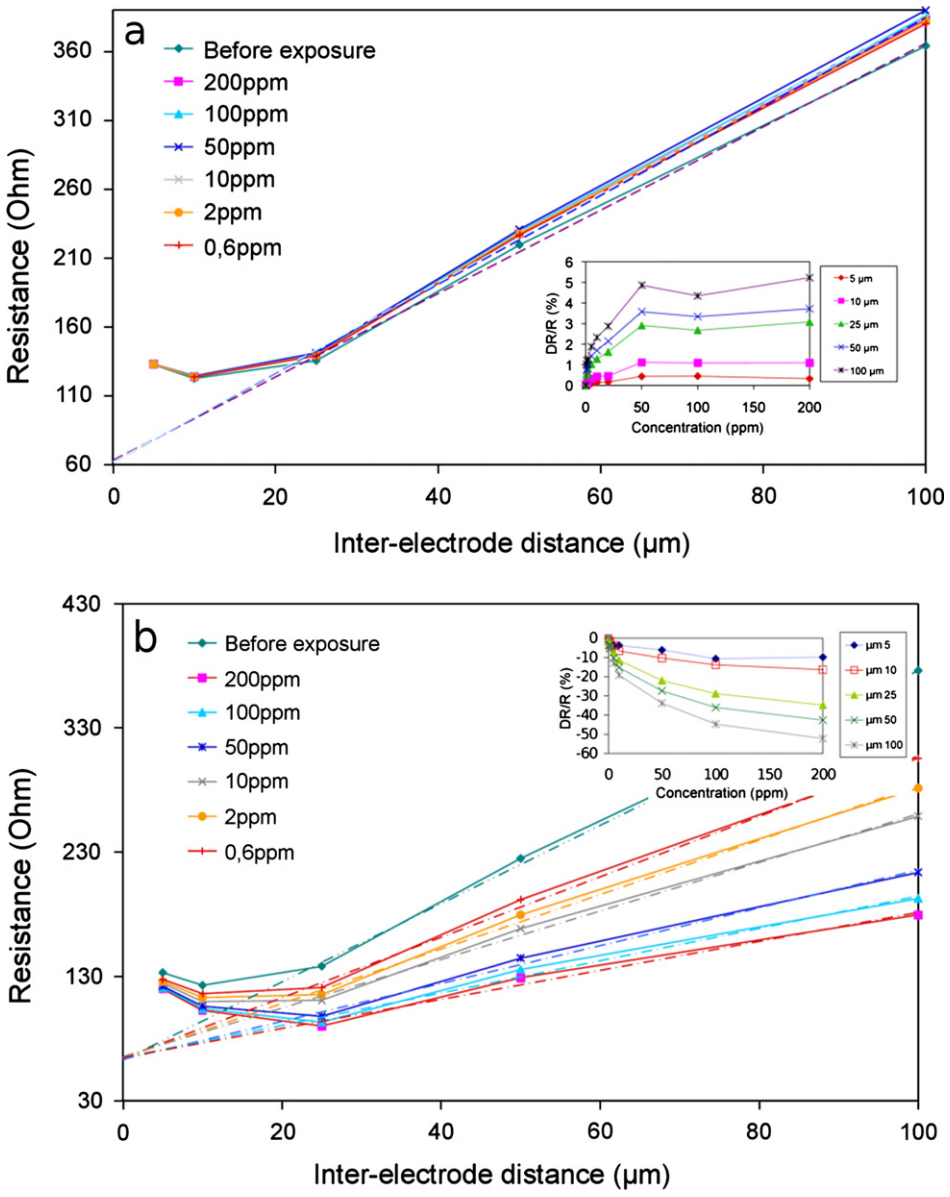

Fig. 9. TLM analysis of the SC-SWCNT film before and after a (a) NH_3 or a (b) NO_2 exposure. In insert, gas concentration vs. the sensor sensitivity.

5. Conclusion

A NO_2 and NH_3 gas sensor is elaborated from sorted SC-SWCNT. The TLM measurements are used in order to deduce the physical sensing mechanism. We have demonstrated that the influence of the target gas on the Schottky barrier is small. It results in a chemisorption of NO_2 and a physisorption of NH_3 on the p-type SC-SWCNT.

References

[1] J. Kong, N.R. Franklin, C. Zhou, M.G. Chapline, S. Peng, K. Cho, H. Dai, Science 287 (2000) 622–625.
[2] Y. Wang, Z. Zhou, Z. Zhang, X. Chen, D. Xu, Y. Zhang, Nanotechnology 20 (2009) 345502.
[3] D.R. Kauffman, A. Star, Angew. Int. Ed. 47 (2008) 6550–6570.
[4] P. Qi, O. Vermesh, M. Grecu, A. Javey, Q. Wang, H. Dai, Nano Lett. 3 (2003) 347–351.
[5] J. Kong, M.G. Chapline, H. Dai, Adv. Mater. 13 (2001) 1384–1386.
[6] P. Bondavalli, P. Legagneux, D. Pribat, A. Balan, S. Nazeer, J. Exp. Nanosci. 3 (2008) 347–356.
[7] M.S. Arnold, A.A. Green, J.F. Hulvat, S.I. Stupp, M.C. Hersam, Nat. Nanotechnol. 1 (2006) 60–65.
[8] S.M. Bachilo, M.S. Strano, C. Kittrell, R.H. Hauge, R.E. Smalley, R.B. Weisman, Science 298 (2002) 2361–2366.
[9] H.Q. Nguyen, J.S. Huh, Sens. Actuators, B 117 (2006) 426–430.

[10] R. Jackson, S. Grahama, Appl. Phys. Lett. 94 (2009) 012109-1–3.
[11] J.-Y. Park, S. Rosenblatt, Y. Yaish, V. Sazonova, H. Ustünel, S. Braig, T.A. Arias, P.W. Brouwer, P.L. McEuen, Nano Lett. 4 (2004) 517–520.
[12] C. Cantalini, L. Valentini, I. Armentano, L. Lozzi, J.M. Kenny, S. Santucci, Sens. Actuators, B 95 (2003) 195–202.
[13] C.W. Bauschlicher, A. Ricca, Phys. Rev. B 70 (2004) 115409-1–6.